Nonlinear Model Predictive Torque Control of a Load Commutated Inverter and Synchronous Machine

Stefan Almér, Thomas Besselmann and Joachim Ferreau
ABB Corporate Research
Segelhofstrasse 1K, 5405 Baden-Dättwil, Aargau, SWITZERLAND
Email: stefan.almer@ch.abb.com

***Abstract*—The paper at hand considers the design of a controller for torque regulation of a variable speed synchronous machine fed by a line commutated rectifier and a load commutated inverter. The control approach is model predictive control where a constrained optimal control problem is solved to minimize the deviation of the torque from its reference. The dynamic model of the converters and drive is nonlinear and considers both the rectifier and inverter firing angles as control input. Controlling both firing angles simultaneously, as opposed to in a cascaded manner, implies improved potential for dynamic performance and disturbance rejection. In particular, the controller handles voltage dips on the line better than a conventional PI controller. The nonlinear MPC solution is implemented through on-line optimization. The optimization algorithm has been implemented on an embedded system and has been shown to execute sufficiently fast for the targeted control frequency.**

I. Introduction

In recent years there has been considerable interest in model predictive torque and/or speed control of variable speed electric machines, see *e.g.,* [1]–[4]. However, the focus of most, if not all, research has been on voltage source converter topologies. In the present paper we consider a synchronous machine fed by *current source* converters. To the best of our knowledge, model predictive control (MPC) has not been applied to this type of system prior to this paper.

The paper considers a variable speed synchronous machine connected to the grid via a line commutated rectifier and a load commutated inverter (LCI) [5], and considers the design of a torque controller. The work is motivated by gas compression plants which are often situated in remote locations and operate under weak grid conditions. Our goal is to design an improved torque controller which can keep delivering torque during partial loss of grid voltage (so-called brown-outs).

Digital Object Identifier: 10.1109/IPEC.2014.6870009

The control approach is set in the framework of MPC. The MPC formulation considers both the rectifier and inverter firing angles as control inputs and stabilizes the DC link current and rotor fluxes while tracking the torque reference. The fact that the rectifier and inverter angles are controlled "simultaneously" rather than in a cascaded fashion implies that the controller has potential for higher dynamic performance compared to conventional approaches. In particular, there is increased potential to deliver torque during brown-outs.

The literature on MPC of power electronics is to a large extent focused on so-called finite control set MPC (FCS-MPC), see *e.g.*, [6]. In FCS-MPC, the control input is restricted to a finite set of values and the MPC problem is solved by enumerating all possible combinations of the input over the prediction horizon. The FCS-MPC approach has a number of drawbacks, including very short prediction horizon, chattering and unpredictable and time varying switching frequency, see [7] for an extensive discussion. The drawbacks of FCS-MPC are mitigated by considering a continuous control variable, such as a duty-cycle or a firing angle, which is mapped to switching action through a modulator. The control approach outlined in the present paper belongs to the later class of methods which considers a continuous control variable.

Implementing the model predictive controller requires to solve a constrained nonlinear, nonconvex optimization problem in real-time. This is a challenging task as our application asks for sampling times of one millisecond or less and the embedded computing power is limited. Solving nonlinear MPC problems in such a situation requires both a careful problem formulation and highly efficient, state-of-the-art optimization algorithms. In this paper, we follow the promising approach of auto-generating customized nonlinear MPC algorithms that are tailored to the problem at hand based on a symbolic problem formulation as proposed in [8].

The paper is organized as follows. In Section II we briefly describe the synchronous machine and the load-commutated inverter. Afterwards a dynamic model of this system is presented in Section III. The developed model predictive torque controller is outlined in Section IV, whereas the state estimation is described in Section V.

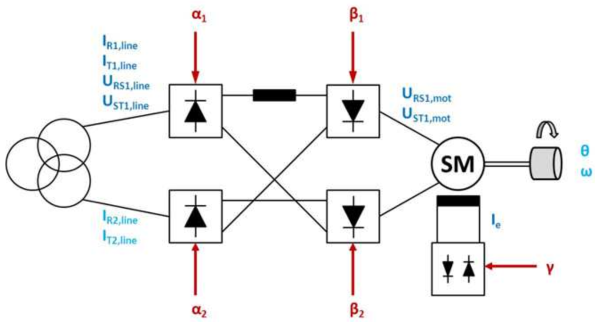

Fig. 1. Variable speed drive system comprised of line commutated rectifier, load commutated inverter and synchronous machine.

Section VI contains simulation results with the proposed controller. Finally conclusions are drawn in Section VII.

II. Current Source Converters and Synchronous Machine

The paper considers a variable speed drive system composed of line commutated rectifiers, inductive DC link, load commutated inverters and a synchronous machine, see Fig. 1. The considered configuration of the converter is a 12/12 pulse setting, whereas the proposed scheme can easily be adapted to other configurations. The shown rectifier and inverter blocks consist of six pulse thyristor bridges. This type of drive systems are suitable for high power applications in the range of several ten's of Megawatts such as high speed compressors or rolling mills.

We note that the synchronous machine has two sets of three phase windings. Each winding pair is connected to its own inverter and both are physically displaced 30^{o} from each other.

The control inputs (signals to be manipulated by the controller) are the firing angles α_1, α_2 of the rectifiers and β_1, β_2 of the inverters. Furthermore, the excitation flux is controlled by an excitation voltage v.

III. Dynamic Model

The rotor excitation flux varies considerably slower than the other states of the system. We therefore control the excitation flux with a slower outer loop and the design of this control loop is not discussed in this paper. The control variable (excitation voltage) v discussed above is therefore not considered in the sequel and the excitation flux is treated as a parameter.

For reduced computational complexity we impose that both rectifiers apply the same firing angles and that both inverters also apply the same firing angles. Thus, the control input is

$$\begin{aligned} \alpha &: \text{ rectifier firing angle} \\ \beta &: \text{ inverter firing angle} \end{aligned}$$

and we impose $\alpha_1 = \alpha_2 = \alpha$ and $\beta_1 = \beta_2 = \beta$.

The state of the system consists of the DC ink current and machine damper windings fluxes:

$$\begin{aligned} \psi_{\mathrm{D}} &: \text{ damper winding flux, d-component} \\ \psi_{\mathrm{Q}} &: \text{ damper winding flux, q-component} \\ i_{\mathrm{DC}} &: \text{ DC link current.} \end{aligned}$$

Using an adaptation of the model of the dual-three phase synchronous machine described in [9] and using an averaged approximation of how the stator currents depend on the inverter firing angle, the dynamics of the damper winding fluxes

$$\Psi := \begin{bmatrix} \psi_{\mathrm{D}} & \psi_{\mathrm{Q}} \end{bmatrix}'$$

are modelled as

$$\frac{d}{dt}\Psi = A\Psi + Bi_{\mathrm{DC}} \begin{bmatrix} \cos(-\beta + \Delta) \\ \sin(-\beta + \Delta) \end{bmatrix} + F\psi_f \,, \qquad (1)$$

where ψ_f is the excitation flux, Δ is the stator voltage angle in the dq-frame and where A, B, F are constant matrices.

The DC link current dynamics are described by

$$\begin{aligned} \frac{d}{dt} i_{\mathrm{DC}} = \frac{1}{L_{\mathrm{DC}}} \Big(& - R_{\mathrm{DC}} i_{\mathrm{DC}} + u_{\mathrm{rec},1} + u_{\mathrm{rec},2} \\ & - u_{\mathrm{inv},1} - u_{\mathrm{inv},2} \Big) \end{aligned} \qquad (2)$$

where L_{DC}, R_{DC} are the inductance and parasitic resistance of the inductor and where $u_{\mathrm{rec,i}}$, $u_{\mathrm{inv,i}}$ are the DC voltages of the rectifier and inverter bridges respectively. We adopt an averaged model to describe the relation between the AC and DC side voltages of the rectifier and inverter. Neglecting the switching and commutation intervals we have

$$u_{\mathrm{rec,i}} \approx kU_L \cos(\alpha), \quad u_{\mathrm{inv,i}} \approx kU_{M,i} \cos(\beta) \qquad (3)$$

where k is a constant, U_L is the amplitude of the line voltages and $U_{M,i}$ are the amplitudes of the stator winding voltages. The line voltage amplitude U_L is a parameter in the MPC problem formulation. The stator voltage amplitudes $U_{M,i}$ of the motor are a (nonlinear) function of the system state. The equations (1)-(3) comprise the dynamic model of the synchronous machine, converters and DC link used in the MPC problem formulation.

A. Torque Expression

The MPC problem formulation penalizes the deviation of the torque from a given reference and we therefore need an expression for the torque. The torque is given by

$$T = (\psi_{d,1} i_{q,1} + \psi_{d,2} i_{q,2} - \psi_{q,1} i_{d,1} - \psi_{q,2} i_{d,2})$$

where $\psi_{d,i}$, $\psi_{q,i}$, $i_{d,i}$, $i_{q,i}$ are the stator fluxes and currents. Using the flux linkage equations and an averaged approximation of how the stator currents depend on the inverter firing angle, the torque can be expressed as a nonlinear function of the system state.

IV. Model Predictive Controller

At each sampling time, the model predictive controller takes an estimate of the system state as initial condition and minimizes a finite time horizon cost integral subject to the dynamic constraints of the system and constraints on the state and input. The cost criterion is

$$J := \int_{kt_\mathrm{s}}^{kt_\mathrm{s}+t_\mathrm{p}} (T - T_\mathrm{ref})^2 dt \tag{4}$$

where t_s is the sampling period, t_p is the prediction horizon length, T_ref is the torque reference.

A. Controller Implementation and On-Line Solution

In order to minimize criterion (4), the corresponding optimal control problem first needs to be discretized in time. If the dynamic model would be linear, one would only need to perform this problem discretization once before the actual runtime of the controller. In that case, the only computational effort to be performed on-line would be solving a convex quadratic programming (QP) problem. Recent years have seen a rapid development of on-line QP solvers that are able to solve such kind of linearized problems in the milli- or even microsecond range on embedded hardware, see *e.g.*, [10]–[13]. Since our model of the drive comprises nonlinear dynamics, we are forced to discretize the optimal control problem on-line at each sampling instant. Along with this discretization in time, we also compute first-order derivatives of the state trajectory with respect to the initial state value and the control moves along the horizon (also called sensitivities). In doing so, we obtain a discrete-time linearization of the optimal control problem, which corresponds to a convex quadratic programming (QP) problem. Finally, we eliminate all state variables from the QP formulation to arrive at a small-scale, dense QP problem. The QP is solved by an adapted variant of the on-line QP solver qpOASES [10]. This procedure to solve nonlinear MPC problems is known as real-time iteration scheme with Gauss-Newton approximation of the second-order derivatives [14].

In order to obtain a highly efficient implementation of the nonlinear MPC algorithm sketched above, we make use of the code generation functionality of the ACADO Toolkit [8], [15]. This software takes a symbolic formulation of the control problem and allows the user to automatically generate customized nonlinear MPC algorithms that are tailored to the specific problem structure. The resulting C code is self-contained, highly optimized and able to run on embedded computing hardware. In our case, the nonlinear MPC controller is running on ABB's controller AC 800PEC, which is based on a 32-bit Power PC processor with a clock speed of up to 600 MHz and also includes an FPGA and a 64-bit IEEE floating point unit. On this platform, the controller has been shown to execute in less than 1 millisecond.

V. State Estimation

The MPC assumes that measurements or estimates of the entire system state are fed to the controller at each sampling time. In the present paper we do *not* assume that the state is measured. Instead, the state is estimated by an observer. The input to the observer corresponds to quantities which are typically measured in an industrial application. This section outlines how the estimates are obtained.

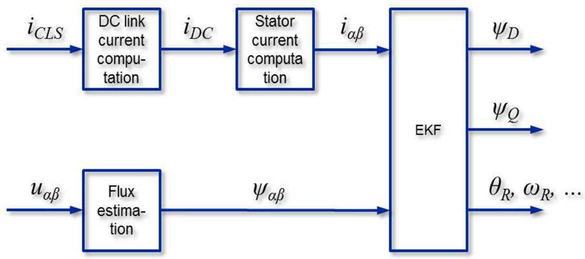

Fig. 2. Structure of the state estimator: Flux estimation and an Extended Kalman Filter.

The available measurements are indicated in Figure 1. While the stator current voltages $u_{\alpha\beta} = [u_\alpha, u_\beta]^T$ are available directly, the DC link current i_{DC} and the stator winding currents $i_{\alpha\beta} = [i_\alpha, i_\beta]^T$ can be deduced from the line side currents and the switching positions of the thyristor bridges.

Figure 2 depicts the structure of the state estimation which consists of two parts; a stator flux estimation and an extended Kalman filter (EKF), [16]. The reason for this separation is that the flux estimator runs at a higher sampling rate in order to increase the estimation accuracy.

The stator flux estimator takes the stator winding currents and voltages in $\alpha\beta$-coordinates and uses the so-called voltage model,

$$u_{\alpha\beta} = R i_{\alpha\beta} + \frac{d}{dt}\psi_{\alpha\beta}\,,$$

to compute an estimate of the stator flux $\psi_{\alpha\beta} = [\psi_\alpha, \psi_\beta]^T$. Using this model, the stator flux is computed by integration.

The stator flux and the stator currents are the inputs to the EKF. The EKF uses a dynamic model of the synchronous machine, similar to the one described in Section III, to estimate the remaining states of the system, in particular the damper winding fluxes $\psi_\mathrm{D}, \psi_\mathrm{Q}$.

VI. Performance Evaluation

The performance of the controller and observer is evaluated in simulation using a high-fidelity Simulink model. The model implements a complex grid model including transformers and harmonic filters. The rectifier, inverter and DC link are implemented using SimPower components and the synchronous machine is represented by a continuous time model derived from first principles. The Simulink model also includes a model of the load which is a rotating mass. The machine considered has rated power of 12 MW and the controller operates with a sampling period of 1 millisecond.

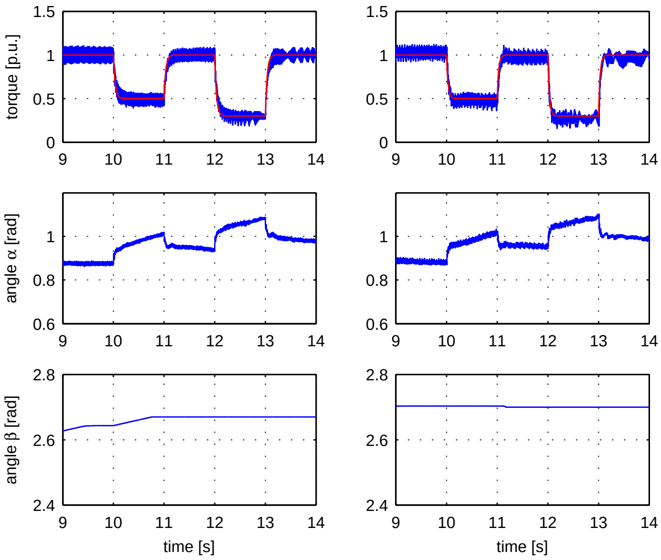

Fig. 3. System response to steps in the torque reference. Left: MPC controller. Right: PI controller.

In the sections below we consider the dynamic performance of the MPC controller and compare it to a state of the art PI-based solution. The prediction horizon of the MPC controller is 20 milliseconds. All signals are represented in the per-unit system.

A. Reference Tracking

We consider the system at nominal steady state and apply steps in the torque reference. The reference, torque and firing angles are shown in Fig. 3 where the left column corresponds to the MPC controller and the right corresponds to the PI controller. It can be seen that both the MPC and PI controller achieve good tracking without overshoot or oscillations. The MPC controller exhibits slightly less variation of the rectifier firing angle α.

B. Line Voltage Drop

We consider the system at nominal steady state and apply steps in the line voltage amplitude. The resulting supply voltage amplitude, torque, DC link current and firing angles are shown in Fig. 4 and 5.

The voltage steps considered have a duration of 0.1 seconds and are spaced one second apart. We consider a sequence of increasingly larger drops. The voltage magnitudes are 0.8 p.u., 0.6 p.u., 0.4 p.u. and 0.2 p.u. (see Fig. 4). This kind of disturbances has been reported to occur when the phases of the transmission line briefly touch due to strong wind.

From Fig. 4 it is clear to see that the voltage steps in the source induces high frequency oscillations in the voltage amplitude seen by the rectifier. This is mainly because the harmonic filters which are present at the side are excited. The results show that the MPC controller manages to keep delivering torque for voltage drops down to 0.4 p.u. For lower drops, the torque goes to zero, but

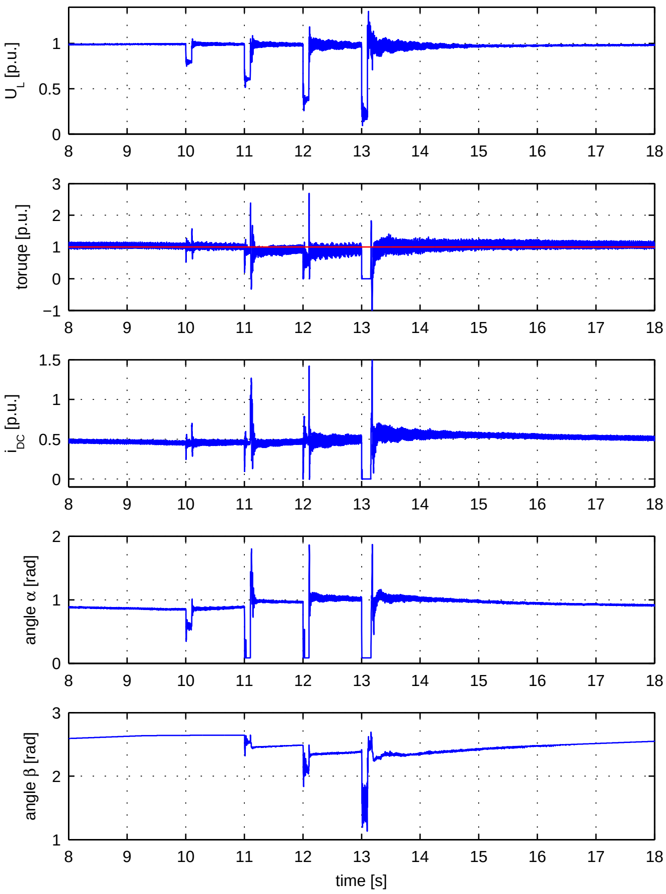

Fig. 4. MPC controller: Response to sudden change in line voltage amplitude.

the system is not destabilized and the torque returns to the reference when the line voltage returns.

The MPC controller is superior to the PI controller which trips already at the first voltage drop down to 0.8 p.u. (see Fig. 5). The PI controller handles the step down in line voltage, but when the voltage returns, the system trips due to a large over-current in the DC-link.

VII. Conclusion

The paper considered nonlinear model predictive control for torque regulation of a synchronous machine supplied by current source converters. The MPC formulation does not impose a cascaded control structure, but uses both the rectifier and inverter angles simultaneously to stabilize the system state and control the torque. This implies increased potential to stabilize the system and reject disturbances. Simulations indeed show that the controller can track the torque reference in the presence of large line voltage drops where a traditional PI controller fails. Thus, the proposed controller increases the system ability of ride-through of brown-outs. Future work could include experimental implementation and development of dynamic models with lower complexity.

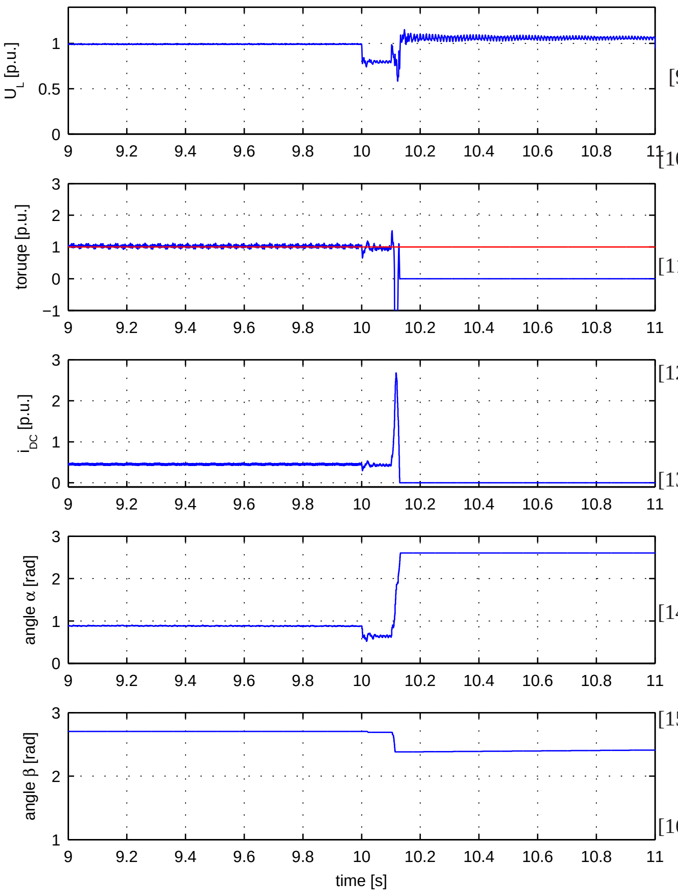

Fig. 5. PI controller: Response to sudden change in line voltage amplitude.

References

[1] S. Mariéthoz, A. Domahidi, and M. Morari. Sensorless explicit model predictive control of permanent magnet synchronous motors. In *IEEE International Conference on Electric Machines and Drives*, pages 1250–1257, 2009.

[2] F. Morel, J.-M. Retif, Xuefang Lin-Shi, and C. Valentin. Permanent Magnet Synchronous Machine Hybrid Torque Control. *Industrial Electronics, IEEE Transactions on*, 55(2):501–511, 2008.

[3] P. Cortes, M.P. Kazmierkowski, R.M. Kennel, D.E. Quevedo, and J. Rodriguez. Predictive control in power electronics and drives. *Industrial Electronics, IEEE Transactions on*, 55(12):4312–4324, 2008.

[4] T. Geyer, G.A. Beccuti, G. Papafotiou, and M. Morari. Model predictive direct torque control of permanent magnet synchronous motors. In *Energy Conversion Congress and Exposition (ECCE), 2010 IEEE*, pages 199–206, 2010.

[5] A. B. Plunkett and F. G. Turnbull. Load-Commutated Inverter/Synchronous Motor Drive Without a Shaft Position Sensor. *IEEE Transactions on Industry Applications*, IA-15(1):63–71, 1979.

[6] S. Kouro, P. Cortes, R. Vargas, U. Ammann, and J. Rodriguez. Model Predictive Control - A Simple and Powerful Method to Control Power Converters. *IEEE Transactions on Industrial Electronics*, 56(6):1826–1838, June 2009.

[7] S. Almér, S. Mariéthoz, and M. Morari. Sampled Data Model Predictive Control of a Voltage Source Inverter for Reduced Harmonic Distortion. *IEEE Transactions on Control Systems Technology*, 21(5):1907–1915, Sept 2013.

[8] B. Houska, H.J. Ferreau, and M. Diehl. An Auto-Generated Real-Time Iteration Algorithm for Nonlinear MPC in the Microsecond Range. *Automatica*, 47(10):2279–2285, 2011.

[9] J. Kaukonen. *Salient Pole Synchronous Machine Modelling in an Industrial Direct Torque Controlled Drive Application*. Phd thesis, Lappeenranta University of Technology, March 1999.

[10] H. J. Ferreau, H. G. Bock, and M. Diehl. An online active set strategy to overcome the limitations of explicit MPC. *International Journal of Robust and Nonlinear Control*, 18(8):816–830, 2008.

[11] J. Mattingley and S. Boyd. *Convex Optimization in Signal Processing and Communications*, chapter Automatic Code Generation for Real-Time Convex Optimization. Cambridge University Press, 2009.

[12] S. Richter, S. Mariéthoz, and M. Morari. High-Speed Online MPC Based on a Fast Gradient Method Applied to Power Converter Control. In *Proceedings of the American Control Conference*, pages 4737–4743, Baltimore, MD, USA, 2010.

[13] A. Domahidi, A. Zgraggen, M.N. Zeilinger, M. Morari, and C.N. Jones. Efficient interior point methods for multistage problems arising in receding horizon control. In *IEEE Conference on Decision and Control (CDC)*, pages 668 – 674, Maui, HI, USA, December 2012.

[14] M. Diehl, H.G. Bock, J.P. Schlöder, R. Findeisen, Z. Nagy, and F. Allgöwer. Real-time optimization and Nonlinear Model Predictive Control of Processes governed by differential-algebraic equations. *J. Proc. Contr.*, 12(4):577–585, 2002.

[15] B. Houska, H.J. Ferreau, and M. Diehl. ACADO Toolkit – An Open Source Framework for Automatic Control and Dynamic Optimization. *Optimal Control Applications and Methods*, 32(3):298–312, 2011.

[16] B.D.O. Anderson and J. Moore. *Optimal Filtering*. Prentice-Hall, Englewood Cliffs, N.J, 1979.